

# MAFT: Efficient Model-Agnostic Fairness Testing for Deep Neural Networks via Zero-Order Gradient Search

Zhaohui Wang  
East China Normal University  
51215902016@stu.ecnu.edu.cn

Min Zhang\*  
East China Normal University  
Shanghai Key Laboratory of  
Trustworthy Computing  
mzhang@sei.ecnu.edu.cn

Jingran Yang  
East China Normal University  
nancyyyyang@163.com

Bojie Shao  
East China Normal University  
51215902099@stu.ecnu.edu.cn

Min Zhang  
East China Normal University  
zhangmin@sei.ecnu.edu.cn

## ABSTRACT

Deep neural networks (DNNs) have shown powerful performance in various applications and are increasingly being used in decision-making systems. However, concerns about fairness in DNNs always persist. Some efficient white-box fairness testing methods about individual fairness have been proposed. Nevertheless, the development of black-box methods has stagnated, and the performance of existing methods is far behind that of white-box methods. In this paper, we propose a novel black-box individual fairness testing method called Model-Agnostic Fairness Testing (MAFT). By leveraging MAFT, practitioners can effectively identify and address discrimination in DL models, regardless of the specific algorithm or architecture employed. Our approach adopts lightweight procedures such as gradient estimation and attribute perturbation rather than non-trivial procedures like symbol execution, rendering it significantly more scalable and applicable than existing methods. We demonstrate that MAFT achieves the same effectiveness as state-of-the-art white-box methods whilst improving the applicability to large-scale networks. Compared to existing black-box approaches, our approach demonstrates distinguished performance in discovering fairness violations w.r.t effectiveness ( $\sim 14.69\times$ ) and efficiency ( $\sim 32.58\times$ ).

## CCS CONCEPTS

• **Computing methodologies** → **Artificial intelligence**; • **Software and its engineering** → **Software testing and debugging**.

## KEYWORDS

software bias, fairness testing, test case generation, deep neural network

\*Corresponding author.

Permission to make digital or hard copies of all or part of this work for personal or classroom use is granted without fee provided that copies are not made or distributed for profit or commercial advantage and that copies bear this notice and the full citation on the first page. Copyrights for components of this work owned by others than the author(s) must be honored. Abstracting with credit is permitted. To copy otherwise, or republish, to post on servers or to redistribute to lists, requires prior specific permission and/or a fee. Request permissions from [permissions@acm.org](mailto:permissions@acm.org).

ICSE '24, April 14–20, 2024, Lisbon, Portugal

© 2024 Copyright held by the owner/author(s). Publication rights licensed to ACM.

ACM ISBN 979-8-4007-0217-4/24/04...\$15.00

<https://doi.org/10.1145/3597503.3639181>

## ACM Reference Format:

Zhaohui Wang, Min Zhang, Jingran Yang, Bojie Shao, and Min Zhang. 2024. MAFT: Efficient Model-Agnostic Fairness Testing for Deep Neural Networks via Zero-Order Gradient Search. In *2024 IEEE/ACM 46th International Conference on Software Engineering (ICSE '24)*, April 14–20, 2024, Lisbon, Portugal. ACM, New York, NY, USA, 12 pages. <https://doi.org/10.1145/3597503.3639181>

## 1 INTRODUCTION

Deep learning (DL) has become an indispensable tool in various domains, including healthcare, finance, weather prediction, image recognition and so on [1–4]. However, as DL models increasingly influence critical aspects of human lives, it has been found that they are vulnerable to slight perturbations [5–8]. In addition to robustness risks, Deep Neural Networks (DNNs) also face fairness threats. DL fairness is a growing area of concern that aims to address bias and unfairness in DNNs.

Discrimination in DNNs may arise from multiple sources, such as biased training data, inadequate features, or algorithmic discrepancies [9]. To detect and evaluate software bias, a growing number of studies have been targeted at group fairness and individual fairness. Individual fairness [10, 11] emphasizes treating similar individuals similarly, regardless of what a protected group they belong to. It evaluates the model on the level of individual instances, which is more fine-grained and can capture subtle biases that may be ignored by the former [11]. Thus we focus on individual fairness to develop methods that can effectively identify and address biases in DNNs at the level of individual instances by generating a large number of individual discriminatory instances. Those instances can be used to retrain models to ease the discrimination of DNNs. There have been several relevant attempts [11–13] on the problem.

In the traditional field of machine learning, existing black-box fairness testing methods perform well. Galhotra et al. proposed THEMIS which randomly samples each attribute in the neighborhood and identifies biased instances to measure the frequency of discrimination [11]. Udeshi et al. first proposed a two-stage global probabilistic search method called AEQUITAS to search discriminatory instances [13]. Agawal et al. proposed a method called Symbolic Generation (SG), which combines two well-established techniques: local interpretability and symbolic execution [14].

However, these methods often shows low efficiency when they struggle to apply to DNNs, given the architectural and algorithmic differences between machine learning and deep learning. The unique challenges posed by DNNs, such as the complexity and

non-linearity of their decision boundaries, demand novel efficient approaches to assess and mitigate biases.

In this case, Zhang et al. proposed a fairness testing approach ADF for DNNs. This approach still combines two-phase generation to search individual discriminatory instances based on input-specific probability distribution which depends on model internal information [15]. Then, Zhang et al. confirmed that ADF is far from efficient, and further proposed EIDIG to systematically generate instances that violate individual fairness. EIDIG inherits and further improves ADF to make it more effective and efficient[16]. However, white-box approaches such as ADF and EIDIG are not applicable in model-agnostic scenarios.

To this end, we propose a novel black-box individual fairness testing method called Model-Agnostic Fairness Testing (MAFT) which can be used in DNN fairness testing without requiring access to their internal workings. MAFT inherits the workflow from EIDIG, so it is almost the same efficient as EIDIG. By converting the use of a real gradient into an estimated gradient, MAFT removes EIDIG's dependency on model, making it a model-independent black-box method for fairness testing of DL. Despite the growing interests in DL fairness, there are only a few black-box fairness methods available that work effectively on deep models, making MAFT a valuable addition to the field.

We have implemented our framework MAFT and compared it with both advanced white-box methods and black-box methods. The overall improvement of MAFT over ADF is 7.92% and 70.77% in effectiveness and separately, consistent with state-of-the-art EIDIG, outperform black-box methods AEQUITAS and SG. MAFT demonstrates a substantial improvement over AEQUITAS and SG, achieving an increase of 1369.42% in effectiveness over AEQUITAS and a 3158.43% enhancement in efficiency compared to SG. These results highlight MAFT's significant advancements in black-box fairness testing domain.

Overall, we make the following main contributions:

- We propose a model-agnostic approach MAFT to do fairness testing for different models without knowing the inner information of models. This versatility allows for broader applications across different DNN systems.<sup>1</sup>
- We evaluate MAFT against white-box methods ADF and EIDIG, along with black-box methods AEQUITAS and SG with 14 benchmarks on seven real-word datasets. The experimental results show that MAFT is almost the same as the state-of-the-art white-box method EIDIG in performance and far outperforms current black-box methods.

## 2 BACKGROUND

### 2.1 Deep Neural Networks

A deep neural network usually contains an input layer for receiving input data, multiple hidden layers for learning, and one output layer for formatting the outputs.

Usually, we can view a trained DNN as a composite function  $F(x)$  and compute its gradient using the chain rule implemented as backpropagation easily. The Jacobian matrix of  $F(x)$  w.r.t a specific

$x$  can be expressed as [16]:

$$J_{F(x)} = \frac{\partial F(x)}{\partial x} = \left[ \frac{\partial F_m(x)}{\partial x_n} \right]_{n \times m} \quad (1)$$

where the  $m$ -th line is the gradient vector of the  $m$ -th output element respect to input data  $x$ .

In many cases, the information within hidden layers of a neural network remains unknown except input data and output confidence, making it intractable for white-box methods such as ADF and EIDIG. However, our proposed approach MAFT solely relies on knowledge of input data and output probabilities to find individual discriminatory instances, yielding excellent performance.

### 2.2 Individual Discrimination

We denote  $X$  as a dataset and its attributes set  $A = \{A_1, A_2, \dots, A_n\}$ . The input domain is denoted as  $I$  and  $I = I_1 \times I_2 \times \dots \times I_n$  if each attribute  $A_i$  has a value domain  $I_i$ . Then we use  $P$  to denote protected attributes of dataset  $X$  like age, race, or gender, and obviously that  $P \subset A$  and use  $NP$  or  $A \setminus P$  to denote non-protected attributes. As for a DNN model trained on  $X$  that may include discrimination, we use  $D(x)$  to denote its output label on  $x$ .

**DEFINITION 1.** Let  $x = [x_1, x_2, \dots, x_n]$ , where  $x_i$  is the value of attribute  $A_i$ , is an arbitrary instance in  $I$ . We say that  $x$  is an individual discriminatory instance of a model  $D$  if there exists another instance  $x' \in I$  which satisfies the following conditions:

- (1)  $\forall q \in NP, x_q = x'_q$ ;
- (2)  $\exists p \in P, x_p \neq x'_p$ ;
- (3)  $D(x) \neq D(x')$ .

Further,  $(x, x')$  is called an individual discriminatory instance pair. Both  $x$  and  $x'$  are individual discriminatory instances.

**EXAMPLE 1.** Let's consider a dataset about person information with 10 attributes, where the gender of a person is chosen as the protected attribute. We have the following pair  $(x, x')$  from the dataset as an example:

$$\begin{aligned} x &: [0, \mathbf{1}, 30, 1, 2, 0, 0, 1, 1, 0] \\ x' &: [0, \mathbf{0}, 30, 1, 2, 0, 0, 1, 1, 0] \end{aligned}$$

We highlight the gender attribute in red for clarity. Except gender,  $x$  and  $x'$  have the same feature. If the decision-making system provides different prediction labels for them, it would be thought as making decisions based solely on gender and ignoring any other attributes. As a result,  $x$  would be considered as an individual discriminatory instance with respect to gender.

### 2.3 Adversarial Attack

Recently, researchers have discovered that DNNs are vulnerable to robustness issues. Even state-of-the-art models can be easily deceived when attackers tamper the original input with minor distortion that are unrecognizable to humans. In light of this, various adversarial attack methods have been proposed to enhance model robustness. These methods have also been found useful in other domains for generating adversarial samples to meet specific requirements, such as fairness testing[15, 16].

Gradient-based adversarial attacks leverage gradients to minimize changes to the input while maximizing changes to the output

<sup>1</sup><https://github.com/wangzh1998/MAFT>

of the sample. In [5], FGSM(Fast Gradient Sign Method) is first proposed as a one-step attack that perturbs the input data by adding small perturbation in the direction of the gradient of the loss function with respect to input according to the following Equation:

$$x^{adv} = x + \epsilon \cdot \text{sign}(\nabla_x L(x, y)) \quad (2)$$

where  $L$  is loss function of  $D$ ,  $y$  is predicted class given by  $D(x)$  and  $\nabla_x L(x, y)$  is gradient of loss function  $L$  on  $x$  w.r.t label  $y$ . The perturbation is scaled by a small value noted by  $\epsilon$  which controls the magnitude of the perturbation and real direction is only determined by the sign of gradient. FGSM is known for its simplicity and effectiveness in generating adversarial examples. Some iterative versions extending FGSM [6, 17] were later proposed. Different from these methods, JSMA(Jacobian-based Saliency Map Attack) [7] adopts the gradient of the model output instead of the loss function, which omits the backpropagation through loss function at each iteration. Inspired by this, a precise mapping between inputs and outputs of DNNs can be established with less time.

In [18], the author proposed a simple black-box adversarial attack. By randomly sampling a vector from a predefined orthonormal basis and then either adding or subtracting it to the target image, the DNN output could be changed. Similar to the setup for training alternative models, the author of [19] proposed a novel black-box attack that also only has access to the input (image) and output (confidence level) of the target DNN. Inspired by this, an efficient vectored gradient estimation method is proposed in our work to guide the generation of discriminatory individual instances.

## 2.4 Fairness Testing Problem Definition

Before introducing a fairness testing problem, we would like to give a formal definition of perturbation on non-sensitive attributes.

**DEFINITION 2.** We use  $x$  to denote the seed input and  $p(x)$  to denote the instance generated from  $x$  by perturbation. We define the perturbation function as follow:

$$p : I \times (A \setminus P) \times \Gamma \rightarrow I$$

where  $\Gamma$  is the set of possible directions for perturbation, e.g.,  $\Gamma$  is defined as  $\{-1, 1\}$  for a single discrete attribute.

A system tends to make discriminatory decision when the system encodes individual discrimination. Based on this, we define fairness testing problem as follow:

**DEFINITION 3.** Given a dataset  $X$  and a DNN model  $D$ , we attempt to generate as many diverse individual discriminatory instances which violates fairness principle in  $D$  (they can be used to mitigate discrimination) by perturbing the seed inputs in the dataset.

## 3 METHODOLOGY

In this section, we present our algorithm called Model Agnostic Fairness Testing (MAFT) for generating individual discriminatory instances. We first describe how to estimate gradient from the black-box model for further gradient-based two-phase algorithm. Then we introduce total workflow of MAFT shown in Fig 1.

### 3.1 Zero-Order Gradient

To leverage the gradient of any general black-box model  $f$  for fairness testing, we employ the asymmetric difference quotient to estimate the gradient.

We first approximate the derivative of function  $f$  with a small constant  $h$ :

$$f'(x) = \lim_{h \rightarrow 0} \frac{f(x+h) - f(x)}{h} \approx \frac{f(x+h) - f(x)}{h} \quad (3)$$

Furthermore, we can extend this expression to the predicted probability vector  $f$  of DNNs whose inputs consist of multi-dimensional features[20]:

$$g_i := \frac{\partial f(x)}{\partial x_i} \approx \frac{f(x + he_i) - f(x)}{h}, \quad (4)$$

where  $g_i$  is the gradient  $\frac{\partial f(x)}{\partial x_i}$  and  $e_i$  is a standard basis vector with  $h$  only the  $i$ -th component set to 1.

So we can get estimated gradient  $\tilde{g}_i$ :

$$\tilde{g}_i := \frac{f(x + he_i) - f(x)}{h} \quad (5)$$

**EXAMPLE 2.** As an illustration of the asymmetric difference formula:  $f'(x) \approx (f(x+h) - f(x))/h$ , we consider a simple one-dimensional function  $f(x) = x^2$  and choose the perturbation size  $h = 0.001$  to compute the estimated gradient of  $f$  at  $x = 2$ . By substituting  $x = 2$  into the difference formula, we can get the estimated gradient value step by step:  $f'(2) \approx (f(2+0.001) - f(2))/0.001 = ((2+0.001)^2 - 2^2)/0.001 = 4.001$ . We can see that the estimate is very close to the real gradient 4 of  $f$  at  $x = 2$ .

**3.1.1 Estimation Error Analysis.** It is important to note that the estimation error is of order  $O(h)$ . We can expand  $f(x + he_i)$  using the first-order Taylor series around  $x$ :

$$f(x + he_i) = f(x) + f'(x) \cdot he_i + O(h^2) \quad (6)$$

where  $f'(x)$  is the first derivative of  $f(x)$ , and  $O(h^2)$  represents all higher-order terms that are of order  $h^2$  or higher. Now, substituting this expansion into the formula of  $\tilde{g}_i$ :

$$\tilde{g}_i = \frac{f(x) + f'(x) \cdot he_i + O(h^2) - f(x)}{h} = f'(x) \cdot e_i + O(h) \quad (7)$$

The estimation error on dimension  $i$  is given by the difference between the true gradient and the estimated gradient:

$$\text{Error} = f'(x) \cdot e_i - \tilde{g}_i = f'(x) \cdot e_i - (f'(x) \cdot e_i + O(h)) = O(h) \quad (8)$$

We can see that the estimation error of the asymmetric zero-order gradient on dimension  $i$  is proportional to  $h$ . This means that the error decreases linearly with the step size  $h$ .

However, the perturbation size  $h$  must be chosen carefully to ensure that the perturbation is not rounded down too much by finite-precision numerical computations in practical phases. Despite concerns about numerical precision, obtaining an accurate gradient estimate is often unnecessary for successful searching. For instance, the FGSM[5] only requires the sign of the gradient, not its exact value, to discover adversarial examples. Thus, even if our initial approximations may lack accuracy, they can achieve high success rates, as demonstrated by our experiments in Section 4.

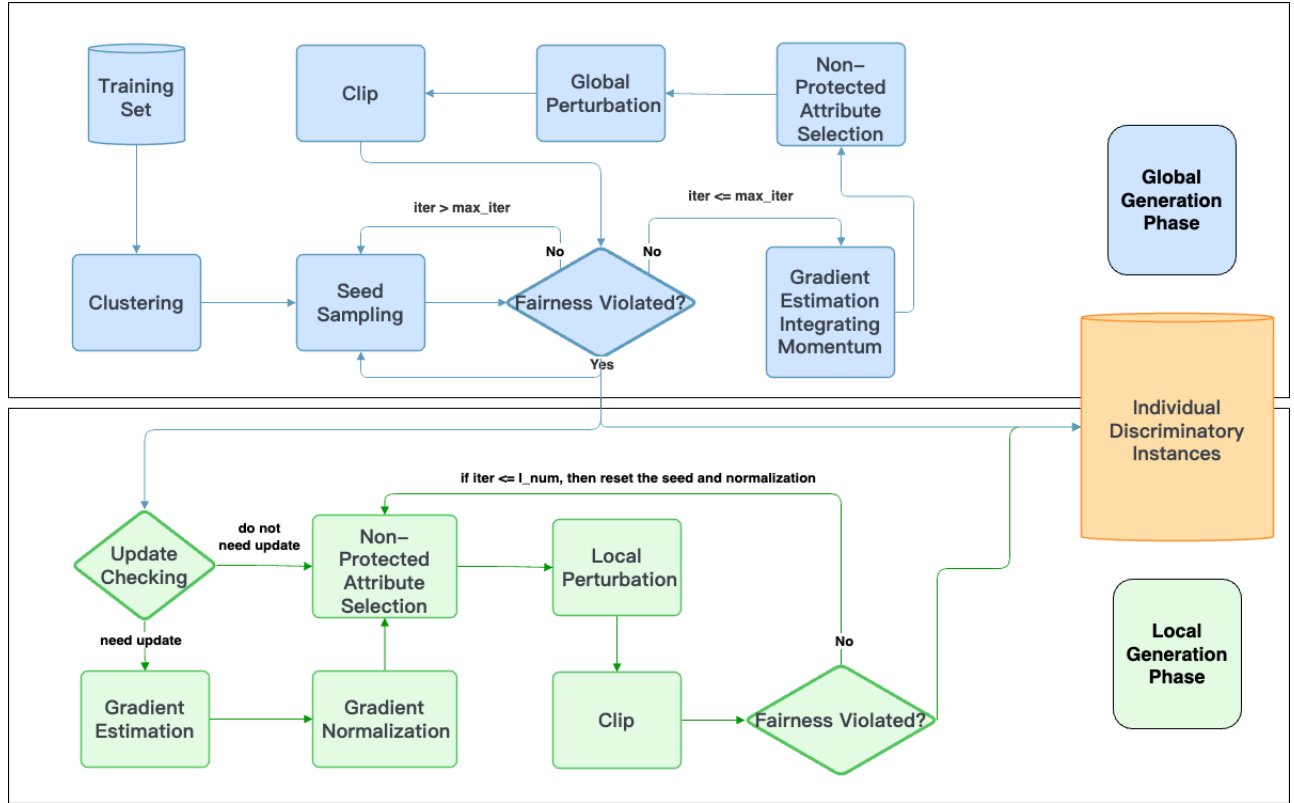


Figure 1: MAFT workflow to generate individual discriminatory instances inherited from EIDIG.

---

**Algorithm 1:** Original Zero-Order Gradient
 

---

**Data:**  $x$ , model,  $perturbation\_size$

**Result:** Estimated Gradient

```

1:  $h \leftarrow perturbation\_size$ 
2:  $n \leftarrow length(x)$ 
3:  $y\_pred \leftarrow model(x)$ 
4:  $gradient \leftarrow$  empty array of size  $n$ 
5: for  $i$  in range  $n$  do
6:    $x\_perturbed \leftarrow copy(x)$ 
7:    $x\_perturbed[i] += h$ 
8:    $y\_perturbed \leftarrow model(x\_perturbed)$ 
9:    $gradient[i] \leftarrow (y\_perturbed - y\_pred)/h$ 
10: if  $model(x) > 0.5$  then
11:   return  $gradient$ 
12: else
13:   return  $-gradient$ 

```

---

**3.1.2 Original Zero-Order Gradient Algorithm.** Based on zero-order gradients, we propose a naive original Non-Vectorized Zero-Order Gradient Algorithm 1. The algorithm aims to estimate the gradient of a given black-box model  $f$  at a given input instance  $x$ . It perturbs each attribute of  $x$  with a specified perturbation step size and then obtains model output corresponding to the perturbed instance (lines 7,8). The finite difference is then used to calculate the gradient in

one dimension (line 9). It proceeds iteratively until gradient values are obtained in all dimensions (lines 5-9).

In this version, gradient estimation for each attribute is calculated in an explicit loop which has obvious drawbacks. Its main disadvantage is computational inefficiency, especially for large models and high-dimensional data, where the computational time required increases linearly with the number of input attributes. If the input instance has  $n$  attributes, the process involves one forward propagation for the original input, followed by  $n$  loops to perform forward propagation for each of the  $n$  perturbed variants. Additionally, differential calculations are performed separately for each variant to obtain the complete gradient, resulting in increased computational overhead. This results in a total of  $n + 1$  forward propagation steps and  $n$  differential calculations. Therefore, it is too slow for real-world applications, especially when dealing with high-dimensional data.

**EXAMPLE 3.** This time, suppose we have a two-dimensional function:  $f(x_1, x_2) = x_1^2 + x_2^2$  and we still use  $h = 0.001$ . If we have an input instance  $x = [x_1, x_2] = [2, 3]$  which has two attributes, we should compute the asymmetric finite difference for each dimension to get the complete estimated gradient: First, we compute  $g_1 \approx (f(x_1 + h, x_2) - f(x_1, x_2))/h$  and then  $g_2 \approx (f(x_1, x_2 + h) - f(x_1, x_2))/h$ . Thus, the zero-order gradient for  $x = [2, 3]$  is  $[4.001, 6.001]$ .

In this example, we only need to compute twice to get the estimated gradient since the function  $f$  has only two attributes ( $x_1$  and

**Algorithm 2: Vektored Zero-Order Gradient****Data:**  $x$ , model,  $perturbation\_size$ **Result:** Estimated Gradient

```

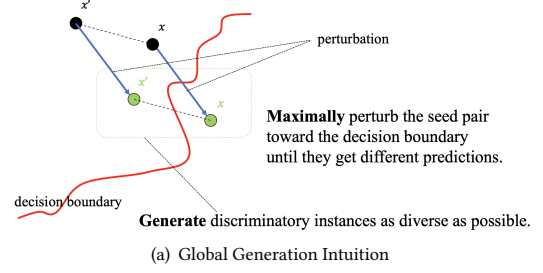
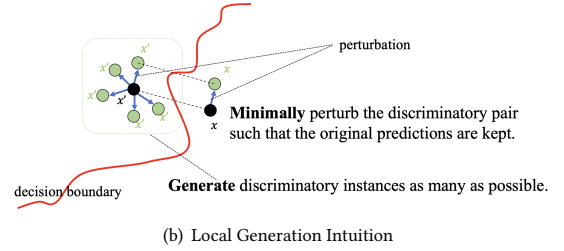
1:  $h \leftarrow perturbation\_size$ 
2:  $n \leftarrow length(x)$ 
3:  $E \leftarrow h \cdot I_n$ 
4:  $X \leftarrow x + E$ 
5:  $Y \leftarrow model(X)$ 
6:  $y\_pred \leftarrow model(x)$ 
7:  $gradient \leftarrow (Y - y\_pred)/h$ 
8:  $gradient \leftarrow reshape(gradient)$ 
9: if  $model(x) > 0.5$  then
10:   return  $gradient$ 
11: else
12:   return  $-gradient$ 

```

$x_2$ ). Note that it consumes much time to get the value of  $f(x_1+h, x_2)$  or  $f(x_1, x_2+h)$  which is a complete forward propagation in deep learning. However, in most scenarios, the number of attributes can be larger, often exceeding ten or even more, which means the entire model must propagate an input ten or more times to estimate the gradient. The efficiency of the original non-vektored algorithm strongly depends on the number of attributes, making it less desirable for high-dimensional input instances. We aim to overcome this limitation by proposing a more efficient vektored zero-order gradient algorithm.

**3.1.3 Vektored Zero-Order Gradient Algorithm.** To overcome the limitations of the original version algorithm and improve computational efficiency, we subsequently introduce more efficient Vektored Zero-Order Gradient in Algorithm 2.

This algorithm takes instance  $x$ , a black-box model and a hyperparameter  $perturbation\_size$  as its input arguments and returns the estimated gradient. We first initialize  $h$  with specified perturbation size and denote the feature numbers of the input instance  $x$  as  $n$  (lines 1,2). If we want to complete the calculation of the entire estimated gradient with only a fixed few times of forward propagation, we'd better obtain the gradient of model output confidence on right class  $p$ , denoted as  $\nabla F_p(x)$ , to a set of variant inputs with different features perturbed at the same time. Note that every element of  $\nabla F_p(x)$  on different features should be independent. To achieve this goal, we first should construct an input square matrix  $X$ , each row of which is a variant of vector  $x$  which has been perturbed on the  $i$ -th feature (lines 3,4). For the model, each row in  $X$  is an independent input instance, so the perturbation of each one has no impact on the results of others. We first construct a diagonal matrix of  $n \times n$ , where the diagonal element value is  $h$  (line 3). It then adds  $x$  row by row to obtain targeted square matrix  $X$  consisting of  $n$  perturbed instances (line 4). In addition to the necessary forward propagation to obtain the black-box model output confidence corresponding to the original input  $x$  (line 6), we only need to perform forward propagation once to obtain the confidence corresponding to each perturbed instance without knowing any internal structure of this model (line 5). Then we use the differential calculation to get a column vector, where each component is the derivative to the

**Global Generation****Local Generation****Figure 2: Two-Phase Generation Intuition**

corresponding perturbation and reshape it to get the zero-order gradient we need (lines 7,8). Finally, we calibrate the sign of the estimated gradient according to whether the confidence is greater than 0.5 (lines 9-12).

The calculation in the above process does not need to rely on any internal information of the model or internal calculation process, it only needs to obtain the confidence level of the model output  $F_p(x)$  in the correct classification  $p$ . Therefore, the above process can be widely used in different scenarios to estimate gradient.

On the other hand, by performing perturbations on entire vectors simultaneously, the vektored version streamlines the computation, leading to better performance. It enables us to estimate the entire gradient with just one or a fixed number of forward propagation, regardless of the number of attributes, which is crucial for practical applications, as it empowers us to efficiently conduct fairness testing and model analysis on large-scale datasets and complex models, making the fairness testing process much more feasible and time-efficient. This efficiency improvement greatly enhances the effectiveness and practicality of our proposed algorithm for fairness testing in real-world deep scenarios.

In essence, the efficiency achieved by the vektored approach brings it close to the computational efficiency of directly utilizing the computational graph for backpropagation, as demonstrated in our experiments as shown in 5(d). This efficiency enhancement is particularly significant for adversarial searching tasks involving black-box models, where computational speed is crucial for effective and timely exploration of potential adversarial examples.

**3.2 Two-Phase Generation**

In this section, we will introduce the workflow of MAFT, which consists of two sequential phases shown as Figure 1 and discuss the

improvement of MAFT by transferring it to the black-box fairness testing domain.

**3.2.1 Global Generation.** Algorithm 3 shows the procedure of global generation. We adopt the global generation phase to accelerate and diversify discrimination generation. The intuition of it is shown in Fig 2(a). We first cluster the original input data set  $X$  with clustering algorithms such as K-means [21] with the goal of discovering diverse instances (line 2). We sample a seed  $x$  from the clusters in a round-robin fashion (line 4). For each selected seed, we perform  $max\_iter$  iterations to find global discriminatory instances (lines 6-21).

According to Definition 1, we need to find an individual discriminatory instance pair to identify an individual discriminatory instance. So we get all instances that differ only in protected attributes from  $x$  as a set  $similar\_x$  (lines 7,8), whose size is the number of all possible combinations of the selected protected attributes in  $I$  except  $x$ . Then we check whether  $x$  violates individual fairness by identifying whether existing individuals in the  $similar\_x$  have different labels with  $x$ . If so,  $x$  can be added to  $global\_id$  as a global discriminatory instance and the iteration stops (lines 9-11). Otherwise, we iteratively perturb  $x$  until a new discriminatory instance is generated or  $max\_iter$  is reached (lines 12-21). We have to find a new discriminatory pair  $(x, x')$ . To solve this problem, EIDIG chooses to traverse  $similar\_x$  to select an instance  $x'$  that

---

**Algorithm 3:** Global Generation

---

**Data:** Training set  $X$ , Attribute set  $A$ , Protected attribute set  $P$ , Input domain  $I$ , model,  $decay$ ,  $max\_iter$ ,  $global\_step$ ,  $cluster\_num$ ,  $global\_num$ ,  $perturbation\_size$

**Result:** Discriminatory Instances

```

1:  $global\_id \leftarrow \emptyset$ 
2:  $clusters \leftarrow \text{Clustering}(X, cluster\_num)$ 
3: for  $i \leftarrow 0$  to  $global\_num - 1$  do
4:   Sample a seed  $x$  from clusters in a round-robin fashion
5:    $grad1 \leftarrow \text{ZerosLike}(x)$ ;  $grad2 \leftarrow \text{ZerosLike}(x)$ 
6:   for  $iter \leftarrow 0$  to  $max\_iter - 1$  do
7:      $similar\_x \leftarrow \{x' \in I \mid \exists a \in P, x'_a \neq x_a;$ 
8:        $\forall a \in (A \setminus P), x'_a = x_a\}$ 
9:     if  $IsDiscriminatory(x, similar\_x)$  then
10:       $global\_id \leftarrow global\_id \cup x$ 
11:      break
12:      $x' \leftarrow \arg \max\{\|model(x) - model(x')\|_2 \mid x' \in$ 
13:        $similar\_x\}$ 
14:      $grad1 \leftarrow decay \cdot grad1 + \text{ComputeGrad}(x)$ 
15:      $grad2 \leftarrow decay \cdot grad2 + \text{ComputeGrad}(x')$ 
16:      $direction \leftarrow \text{ZerosLike}(x)$ 
17:     for  $a \in (A \setminus P)$  do
18:       if  $sign(grad1[a]) = sign(grad2[a])$  then
19:          $direction[a] \leftarrow (-1) \cdot sign(grad1[a])$ 
20:      $x \leftarrow x + global\_step \cdot direction$ 
21:      $x \leftarrow \text{Clip}(x, I)$ 
22: return  $global\_id$ 

```

---

has the biggest difference in model output with  $x$  (lines 12,13) because the intuition is that  $x$  and  $x'$  are more likely to be separated by the decision boundary of the model after perturbation if the Euclidean distance between their model predictions is maximized. Then, we perturb  $x$  and  $x'$  simultaneously on non-protected attributes to make one of them cross the decision boundary in the opposite direction of the gradient by decreasing the model prediction confidence on their original label (lines 16-20). Momentum [22] is used as an optimization method for speeding up the procedure by accumulating local gradient and increasing efficiency, because it can help stabilize update and escape from local minimum or maximum [23] (lines 14,15).

EIDIG constructs a direct and precise mapping from input feature perturbation to output variation, which should be done by internal backpropagation of model for gradient calculation. However, we replace this computation of  $\nabla_x F_p(x)$  with our estimated gradient shown as  $ComputeGrad(x)$  to make this method independent of the model itself.

At last, we clip the generated instance  $x$  to keep it within the input domain  $I$  (line 21). Finally, this algorithm returns all generated discriminatory instances (i.e.,  $global\_id$ ) which will be used as the seed inputs for local generation phase.

**3.2.2 Local Generation.** Algorithm 4 shows the contents of local generation phase, which quickly generates as many discriminatory instances as possible around the seeds  $global\_id$  generated by the global generation phase. The intuition of it is shown as Fig 2(b).

Unlike the global phase, which maximizes output variation to discover potential individual discriminatory instance pairs at each iteration, the local phase focuses on changing model variation to maintain the original predictions from the model. In doing so, we could get more similar discriminatory instances, which is motivated by DNN robustness that similar inputs lead to similar or the same outputs [8, 24]. For this, we just need slight perturbation on the local phase.

For each global seed from  $global\_id$ , there must be a similar instance  $x'$  which has different label (lines 6-8). Then we also use gradient information to guide attribute selection and perturbation (lines 9-11, 14-17). To keep the prediction, we prefer to select an attribute that has less impact on the model, and thus the instance can keep the same label after perturbation. We calculate normalized probabilities of non-protected attributes as attribute contribution according to reciprocals of their gradients (line 11). Then we use this probability to choose an attribute to perturb on random direction  $s$  (lines 14-17), because we tend to choose an attribute that has less impact on the model after perturbation. If  $x$  becomes a new discriminatory instance after perturbation, we add it to  $local\_id$  set (lines 21,22). Otherwise, we reset  $x$  and corresponding probability to next iteration. EIDIG shows that the information guiding attribute selection and perturbation is likely to be highly correlated at each iteration due to small perturbation in the local generation phase, so it chooses to calculate the attribute contributions every few iterations (lines 5-12).

During this phase, EIDIG still use  $\nabla_x F_p(x)$  to establish a direct and precise mapping from input perturbation to output variation on original right label  $p$  to compute normalized probability. However, we replace this computation of  $\nabla_x F_p(x)$  with our estimated

**Algorithm 4:** Local Generation

---

**Data:** Attribute set  $A$ , Protected attribute set  $P$ , Input domain  $I$ ,  $local\_num$ ,  $global\_id$ ,  $model$ ,  $update\_interval$ ,  $local\_step$

**Result:** Discriminatory Instances

```

1:  $local\_id \leftarrow \emptyset$ 
2: for  $x \in global\_id$  do
3:    $suc\_iter \leftarrow update\_interval$ 
4:   for  $iter \leftarrow 0$  to  $local\_num - 1$  do
5:     if  $suc\_iter \geq update\_interval$  then
6:        $similar\_x \leftarrow \{x' \in I \mid \exists a \in P, x'_a \neq x_a;$ 
7:          $\forall a \in (A \setminus P), x'_a = x_a\}$ 
8:        $x' \leftarrow \text{FindPair}(x, similar\_x, model)$ 
9:        $grad1 \leftarrow \text{ComputeGrad}(x)$ 
10:       $grad2 \leftarrow \text{ComputeGrad}(x')$ 
11:       $probability \leftarrow \text{Normalization}(grad1, grad2, P)$ 
12:       $suc\_iter \leftarrow 0$ 
13:       $suc\_iter \leftarrow suc\_iter + 1$ 
14:       $a \leftarrow \text{RandomPick}(probability)$ 
15:       $direction \leftarrow (-1, 1)$ 
16:       $s \leftarrow \text{RandomPick}([0.5, 0.5])$ 
17:       $x[a] \leftarrow x[a] + direction[s] \cdot local\_step$ 
18:       $x \leftarrow \text{Clip}(x, I)$ 
19:       $similar\_x \leftarrow \{x' \in I \mid \exists a \in P, x'_a \neq x_a;$ 
20:         $\forall a \in (A \setminus P), x'_a = x_a\}$ 
21:      if  $IsDiscriminatory(x, similar\_x)$  then
22:         $local\_id \leftarrow local\_id \cup x$ 
23:      else
24:         $\text{Reset}(x); \text{Reset}(probability)$ 
25:         $suc\_iter \leftarrow 0$ 
26: return  $local\_id$ 

```

---

gradient shown as  $\text{ComputeGrad}(x)$  again to make this method independent of the model itself (lines 9,10).

At this time, we have generated a large number of individual discriminatory instances, which can be used for retraining to remove bias from the original model.

## 4 IMPLEMENTATION AND EVALUATION

In this section, we present experiments designed to evaluate the performance of MAFT and explore why estimated gradient is effective and efficient. The experiments can be structured into three primary research questions (RQs):

- RQ1:** How does the choice of hyperparameter affect the performance of MAFT?
- RQ2:** Given the selected hyperparameter, how does MAFT compare with AEQUITAS, ADF and EIDIG in terms of effectiveness and efficiency?
- RQ3:** To what extent does the estimated gradient in MAFT match the real gradient in EIDIG in terms of effectiveness and efficiency?

**Table 1: Comparing different methods.**

	THE	AEQ	SG	ADF	EIDIG	MAFT
Effective & Efficient	×	×	×	✓	✓	✓
Model-agnostic	✓	✓	✓	×	×	✓

**Table 2: Benchmark Datasets and Model Accuracy**

Dataset	#Ins	#Fea	Protected Attrs	Accuracy
Bank Marketing <sup>2</sup>	45211	16	Age	89.22%
Cencus Income <sup>3</sup>	48422	12	Age Race Gender	84.32%
German Credit <sup>4</sup>	1000	24	Age Gender	78.25%
Diabetes <sup>5</sup>	768	8	Age	74.03%
Heart Heath <sup>6</sup>	297	13	Age Gender	74.79%
MEPS15 <sup>7</sup>	15830	137	Age Race Gender	84.55%
Students <sup>8</sup>	1044	32	Age Gender	86.6%

### 4.1 Experimental Setup

*Baselines.* According to the features of different methods that are shown in Table 1 (THE and AEQ are the abbreviation of THEMIS and AEQUITAS separately), we can know that model-agnostic methods such as AEQUITAS and SG are ineffective and inefficient. To answer these questions, we select to utilize AEQUITAS, SG, ADF and EIDIG as baseline comparison techniques. As THEMIS is shown to be significantly less effective [14] and thus is omitted. Through comparison with black-box methods, we demonstrate the superior performance of MAFT. Additionally, by contrasting it with white-box methods, we highlight why it have distinct advantages and strengths.

In addition to this, we have to highlight that MAFT differs from ADF and EIDIG by operating as a black-box approach, so retraining is unnecessary to demonstrate the effectiveness of the discriminatory instances generated. If you wish to confirm the effectiveness of these instances in retraining to alleviate the model's bias, you are encouraged to refer to ADF and EIDIG.

*Datasets and Models.* To evaluate MAFT, we select seven benchmark datasets that have been used in previous studies [11, 13–16]. The details are as Table 2 (#Ins means number of instances, #Fea expresses the number of features and *Protected Attrs* are protected features).

The predictive tasks based on these datasets center around determining whether an individual meets certain conditions. Owing to the simplicity of these datasets, we employ the six-layer fully connected networks that was adopted by EIDIG. The details of the models' accuracy are shown in Table 2. Prior to the tasks' beginning, it was necessary to preprocess the data particularly in regard to the conversion of continuous attributes into categorical ones. For instance, we discrete age based on human lifecycle. For ease of denotation, each benchmark was denoted as "B-a", where "B" represents the initial uppercase letter of the dataset, and "a" refers to the initial lowercase letter of the sensitive attribute.

*Configurations.* Both ADF and EIDIG are configured according to the best performance setting reported in the respective papers. For global, max iteration  $max\_iter$  is set to 10 because less than 5

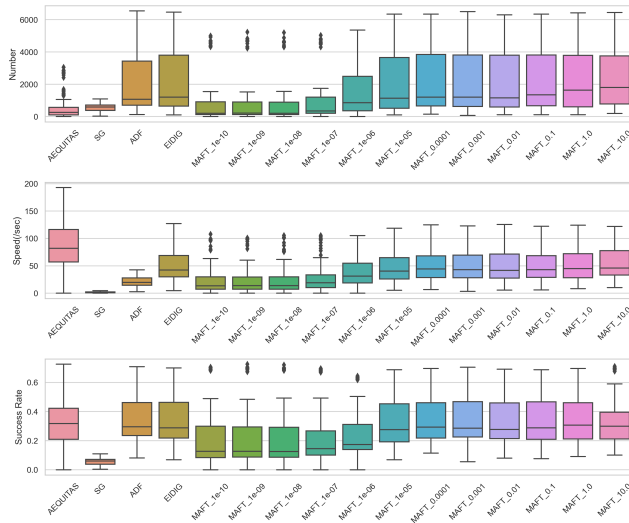


**Figure 3: Hyperparameter: Perturbation Size Comparison**

iterations need to be taken for most situations to find an individual discriminatory instance around the seed if there exists and both global step size *global\_step* and local step size *local\_step* are set to 1.0, i.e., the minimum step for the categorical attributes. During global phase, we set cluster count *cluster\_num* to 4 as ADF and EIDIG did to cluster the training set using K-Means [21]. As EIDIG achieves best performance when past gradient information decays away to half its origin after each iteration, we set decay factor of momentum *decay* to 0.5. During local phase, we set prior information life cycle *update\_interval* to 5 to make a balance of prior information effectiveness and update frequency. As for perturbation size *perturbation\_size*, we will discuss it in 4.2.1.

We re-implemented SG and AEQUITAS using TensorFlow 2 and make slight adjustments to make them having the same maximum search iterations with white-box methods under same parameters. We opt for a fixed random seed to generate initial input for AEQUITAS in input domain to keep stability. Other settings are also kept best.

All experiments were run on a personal computer with 32 GB RAM, Intel i5-11400F 2.66GHz CPU and NVIDIA GTX 3060 GPU in Ubuntu22.04

## 4.2 Results and Discussion

Notice that besides AEQUITAS, all of ADF, EIDIG and MAFT share a similar gradient-based testing framework with two sequential phases. To this end, we compare them phase by phase to answer these research questions.

**4.2.1 Hyperparameter Study: Perturbation Size (RQ1).** The perturbation size  $h$  is a critical hyperparameter in MAFT. In this experiment, our goal is to provide valuable insights for the effects of perturbation size and determine the optimal perturbation size for the MAFT method across various benchmarks in the settings of tabular data. In these experiments,  $g\_num$  and  $l\_num$  were set to 100 and 100 separately (in the formal experiments, they were set to 1000 and 1000). We performed experiments on multiple benchmarks using five different methods: MAFT with various perturbation size values ranging from  $1e - 10$  to 10, AEQUITAS, SG, ADF and EIDIG, each with their optimal parameters. Specifically, the methods included MAFT, varying across 12 parameter configurations, thus yielding a total of 16 methods of distinct settings. Each unique combination underwent rigorous evaluation through 10 rounds. Subsequently, we aggregated the resultant data points for each method and plotted them with a boxplot shown in Fig 3.

In Fig 3, vertical axes in different subfigures represent instance generation number, instance generation speed, and success rate for generating discriminatory instances in effective attempts separately. Notice that higher values are better for all of the three metrics alone. The horizontal axis represents AEQUITAS, SG, ADF, EIDIG, and MAFT with different perturbation size values. We get several observations from the results. AEQUITAS adopts a global adaptive search strategy, which continuously reinforces past successful choices during search. In doing so, AEQUITAS is more inclined to exploit than to explore, and thus it sticks in duplicate search paths, resulting in finding much less fairness violations, even if it achieves good performance in terms of generation speed and success rate due to its heuristic nature. SG is both ineffective and inefficient, because it heavily relies on the existing techniques about local explanation and symbolic execution, which are both time-consuming. Specifically, MAFT with  $h = 1$  generates 292.15% more biased samples than SG at 3158.43% higher speed on average. EIDIG significantly outperforms ADF especially in speed. Moreover, the success rate of EIDIG is slightly lower than ADF, since EIDIG doesn't utilize completely accurate gradients in most iterations during local search, but EIDIG explores much more search space owing to its momentum integration during global search. For MAFT, when  $h$  is less than or equal to  $1e - 6$ , the results are even significantly inferior to ADF. However, the results improve as  $h$  increases within the range of  $(1e - 8, 1e - 5]$  and keep increasing until the metrics remain relatively stable within the range of  $(1e - 5, 10]$  with the number and speed metrics comparable with EIDIG. We apply ANOVA[25] to verify that the experimental results of MAFT with  $h$  in  $(1e-5, 10]$  do not exhibit statistically significant differences. At  $h = 1$  and  $h = 10$ , we get the highest average number and speed, but the success rate at  $h = 10$  obviously drops. These results demonstrate that when  $h$  is too small, the perturbation is so subtle that it fails to estimate a useful gradient. Conversely, when  $h$  is too large, the estimated gradient deviates significantly. When  $h$  is kept at an appropriate value, the experimental effects are relatively stable and efficient.

Overall, we recommend using the perturbation size of 1, and it is also the minimum granularity of the preprocessed attributes of the subject tabular datasets after discretization. We also encourage users to try to choose parameters that are more suitable for their specific datasets.

<sup>2</sup><https://archive.ics.uci.edu/ml/datasets/bank+marketing>

<sup>3</sup><https://www.kaggle.com/vivamoto/us-adult-income-update?select=census.csv>

<sup>4</sup><https://dataverse.harvard.edu/dataset.xhtml?persistentId=doi:10.7910/DVN/Q8MAW8>

<sup>5</sup><https://archive.ics.uci.edu/ml/datasets/diabetes>

<sup>6</sup><https://archive.ics.uci.edu/ml/datasets/Heart+Disease>

<sup>7</sup><https://github.com/HHS-AHRQ/MEPS>

<sup>8</sup><https://archive.ics.uci.edu/ml/datasets/Student+Performance>



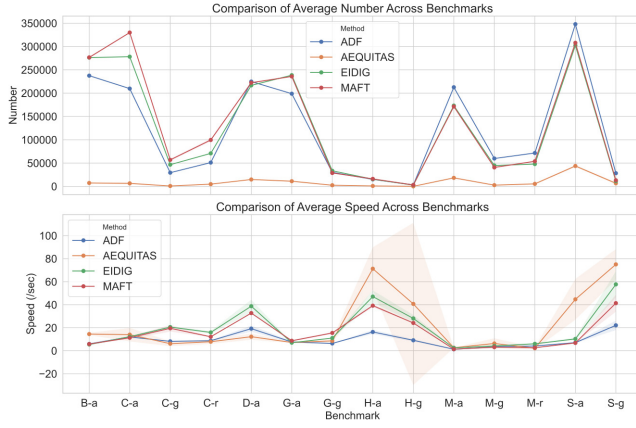


**Figure 4: Individual Discriminatory Instance Generation Comparison**

In a certain range, the influence of perturbation magnitude is stable. In practical applications, we can choose the optimal parameters on demand. For simplicity, we recommend using the perturbation size of 1 for preprocessed tabular datasets with discret attributes.

**4.2.2 Comprehensive Results: Effectiveness and Efficiency (RQ2).** After selecting the hyperparameter, we compare the overall performance of MAFT to the baselines such as AEQUITAS, ADF and EIDIG, considering both the quantity of generated test cases which means **effectiveness** and the generation speed which means **efficiency**. Note that we exclude SG because it is too time-consuming.

Following the setting established by EIDIG, we select 1000 instances from clustered dataset as inputs for global generation, and subsequently generate 1000 instances in the neighbourhood of each global discriminatory seed during local generation (i.e.,  $g\_num = l\_num = 1000$ ). Note that some datasets are small which number of instances are less than 1000, so we utilize the whole training set as seeds for global generation. For each benchmark, we run three rounds and average the results. The comparison results are displayed in Fig 4, where we plot the average results with line charts and mark the fluctuation ranges with shading. The first subfigure illustrates the number of individual discriminatory instances generated by each approach, whereas the second subfigure demonstrates the number of individual discriminatory instances generated per second. The MAFT lines are largely consistent with the EIDIG lines, and both achieve comparable effectiveness and much better efficiency than ADF. We further apply t-tests [26] to these methods pairwise. There is no statistically significant difference between the results of effectiveness of ADF, EIDIG, and MAFT, and there is also no statistically significant difference in efficiency of EIDIG and MAFT.

Specifically, MAFT generates 1369.42% more discriminatory samples with 28.41% lower speed when compared with AEQUITAS, 7.92% more discriminatory samples with 70.77% higher speed when compared with ADF, and 5.58% more discriminatory samples with 15.91% lower speed when compared with EIDIG. Despite avoiding the direct computation of gradient depending on the model, our approach demonstrates an excellent performance in generating

individual discriminatory instances. As a black-box method, AEQUITAS achieves outstanding performance w.r.t efficiency, but its speed is extremely unstable. Moreover, AEQUITAS generates much less biased samples than the white-box methods, which fails to fully expose the fairness issues of the tested DNNs. Our results are consistent with the results from [15], which prove that AEQUITAS turns inefficient under a target of generating numerous biased samples.

As to why the estimated gradients achieve similar results to the real gradients in EIDIG in terms of effectiveness and efficiency, We will explore further in the following experiments.

**In conclusion, MAFT matches the performance of the state-of-the-art white-box method EIDIG, significantly outperforms another white-box method ADF, and markedly surpasses other black-box methods like SG and AEQUITAS.**

**4.2.3 Gradient Validation (RQ3).** This question aims to highlight the effectiveness and efficiency of MAFT’s gradient estimation procedure by mainly comparing with EIDIG. We not only compare the gradient itself, but also compare the gradient directions and normalized probabilities computed and used by MAFT and EIDIG at both the global and local stages.

The sub-questions in RQ3 are:

**RQ3.1:** How similar are the estimated gradient of the MAFT and the real gradient of other methods, and how similar are their costs in terms of computational time?

**RQ3.2:** In the global stage, how similar are the guidance directions of the perturbations calculated using the gradient of MAFT and EIDIG, and how similar are their costs in terms of computational time?

**RQ3.3:** In the local stage, how similar are the normalized probabilities of perturbation calculated using the gradients of MAFT and EIDIG, and how similar are their costs in terms of computational time?

We use cosine similarity as a metric. For two vector  $\vec{A}$  and  $\vec{B}$ , the cosine similarity are defined as:

$$\text{cosine similarity}(\vec{A}, \vec{B}) = \frac{\vec{A} \cdot \vec{B}}{\|\vec{A}\| \times \|\vec{B}\|} \quad (9)$$

which  $\vec{A} \cdot \vec{B}$  is dot product and  $\|\vec{A}\| \times \|\vec{B}\|$  is product of vector modules. For RQ3.1, we conduct separate experiments to compare the functions for gradient calculation and estimation. For each benchmark, we randomly select 1000 seeds (or whole small dataset as seeds) from the original dataset. The similarity between the real gradient and the estimated gradient for each seed is then calculated. The results are presented in Fig 5(a).

Regarding effectiveness, it is observed from Fig 5(a) that the average gradient similarity across the majority of benchmarks is above 0.8 and the distribution of them concentrate at the top value (about 1) of the violin graph, which means the compactness of their distribution. This result confirms that the simulated gradient can provide sufficient guidance for exploring the input space and identifying various discriminatory instances.

We also process the gradients to project them onto a two-dimensional space through Principal Component Analysis (PCA) [27] and illustrate the intuitive result in Fig 6 which axes represent the principal components of PCA. This visualization effectively demonstrates

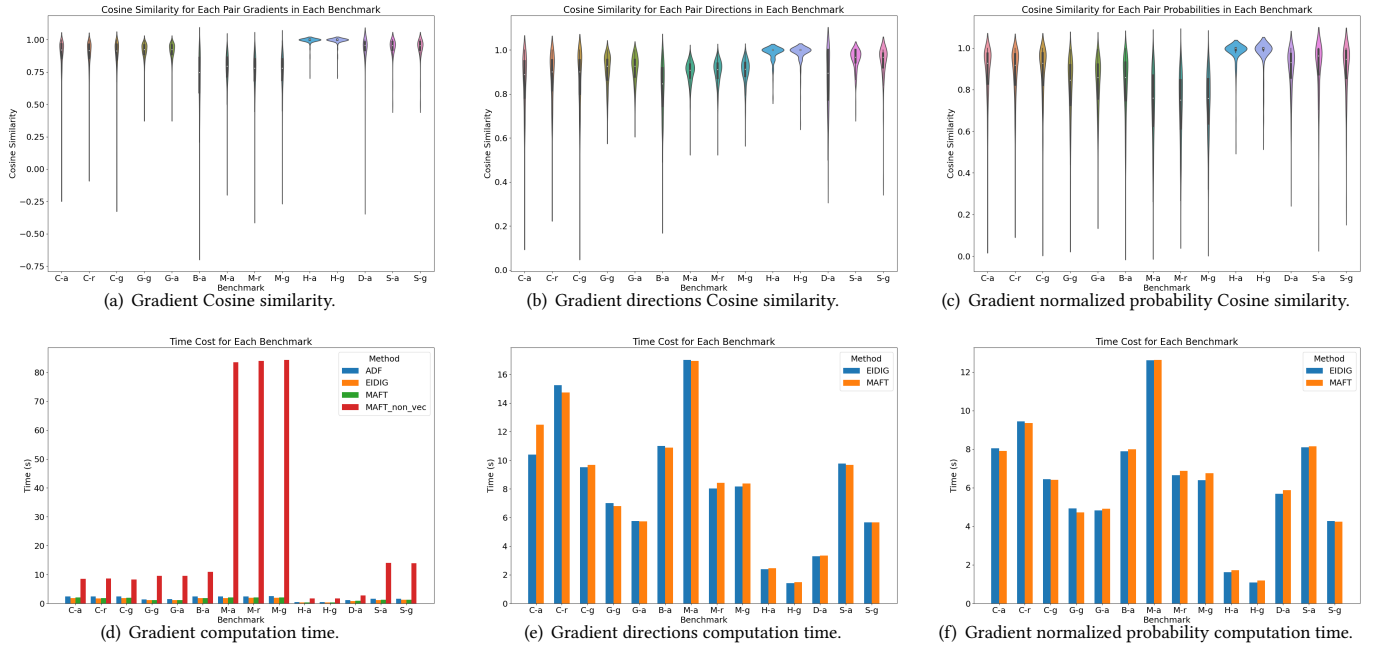


Figure 5: Gradient : Comprehensive Comparison

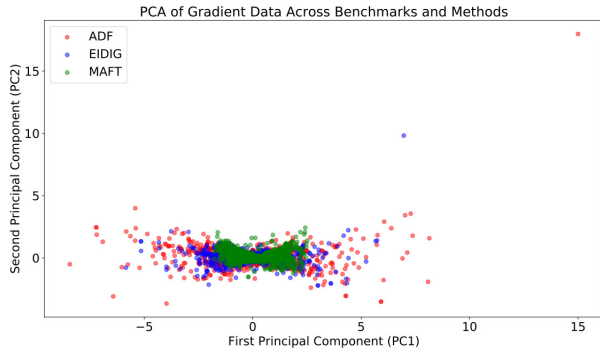


Figure 6: Gradient PCA Comparison

the close alignment of gradients produced by MAFT with those from EIDIG, and a distinct deviation from the gradients generated by ADF due to the transformation from loss gradients to output probability gradients.

Regarding efficiency, Fig 5(d) displays the time consumption for ADF, EIDIG, MAFT and MAFT\_non\_vec (MAFT\_non\_vec uses original estimation algorithm shown as Algorithm 1). MAFT\_non\_vec costs excessive amount of time on MEPS15, because MEPS15 has over 100 attributes, which are much more than those of others. EIDIG is noticeably faster than ADF which can be attributed to the absence of the backpropagation through the loss function. Why MAFT takes slightly more time than EIDIG, but the performance is almost the same? The calculation of 1000 gradients costs less than 10 seconds (except MAFT\_non\_vec), which is a relatively minor part of the entire exploration. This will be shown obviously in next

two comparisons. The time cost difference between MAFT and EIDIG is negligible considering the entire exploration process.

*Time Complexity Analysis of Gradient Estimation.* Let's recall the process of getting real gradient by backpropagation (BP): First, backpropagation requires once forward propagation (FP) to compute the output  $f(x)$ . Second, it requires once backward propagation to compute the gradients of the loss (ADF) or output value (EIDIG) w.r.t a specific input. So the complexity for this step is  $O(FP + BP)$ . While in estimation algorithm, we can forward propagate twice on the input  $X$  and  $x$  separately through the model to compute zero-order gradient. The time complexity for this step is just  $O(2*FP)$  ignoring fixed computation operations. Subtracting the common forward propagation step of those two methods, we can focus on remaining computational efforts with the vectored zero-order gradient method at  $O(FP)$  and backpropagation at  $O(BP)$ . It's obvious that forward propagation should just through the model of the input layer to output layer in the forward direction. According chain rule, backpropagation computes gradients directly for each layer, requiring only a single pass through the model in the opposite direction from forward propagation. The relationship between  $O(FP)$  and  $O(BP)$  depends on the specific model and implementation, but typically,  $O(FP)$  and  $O(BP)$  are of similar orders of magnitude since both methods involve traversing the layers of model once.

Next, regarding RQ3.2 and RQ3.3, further exploration is conducted on the directions and normalized probabilities of perturbation that serve to guide exploration during the global and local stages, respectively.

In the case of RQ3.2, we solely compare the consistency of direction information used in the first iteration of global generation. For each benchmark, we randomly select 1000 seeds (or whole small

dataset as seeds). For each instance  $x_1$  from the seeds, we identify its most dissimilar instance  $x_2$  from the similar set which contains all instances that differ only in protected attributes from  $x_1$ , to construct a pair  $(x_1, x_2)$ . If they are a pair of discriminatory instances, they will be ignored as there is no need for further global search. Otherwise, we calculate their real gradients denoted as  $(g_1, g_2)$  and estimated gradients denoted as  $(\tilde{g}_1, \tilde{g}_2)$ . Subsequently, we obtain the real gradient direction  $d$  by comparing the signs of  $g_1$  and  $g_2$ , and estimated gradient direction  $\tilde{d}$  by comparing  $\tilde{g}_1$  and  $\tilde{g}_2$ . The iteration continues until completion for each seed, resulting two sets of real directions and their corresponding estimated directions, respectively. The similarity between these real directions and estimated directions is further computed and compared.

As for RQ3.3, we compare the consistency of normalized probability information used in local generation. We use randomly collected 1000 seeds instead of globally discriminatory instances as inputs and construct pairs for them like RQ3.2. Subsequently, we independently calculate the real and estimated gradients for the paired instances. Following this, we compute the normalized probabilities denoted as  $p$  and  $\tilde{p}$ , used in selecting the perturbation attributes. The similarity of them is also computed and compared.

We find that the similarity of perturbation directions and the similarity of normalized probabilities are highly consistent with the similarity of gradients, which means the fine-grained usage of estimated gradient is still useful. The cosine similarity distribution of gradient directions in Fig 5(b) is consistent with that in Fig 5(a), so is it in Fig 5(c).

The time comparison in Fig 5(e) and Fig 5(f) demonstrate that when considering both gradient calculation and other computational operations within a single iteration, the time difference between EIDIG and MAFT further decreases.

**In summary, the experimental results from RQ3.1 to RQ3.3 convincingly demonstrate that the estimated gradient closely matches the real gradient in terms of both efficiency and effectiveness.**

### 4.3 Threat to Validity

*Internal Validity.* We take average of repeated experiments to ensure the validity of our conclusion. We consider only one sensitive attribute as each benchmark for our experiments. Actually, we have experimentally verified that MAFT remains superior to the other methods considering multiple sensitive attributes. All methods relatively generate more biased samples with more execution time in such circumstances, since all the possible combinations of their unique values need to be checked.

*External Validity.* Our black-box method is naturally applicable to more scenarios than white-box methods, and the gradient estimation technique of MAFT could be combined with follow-up testing frameworks based on gradient. To ensure the generalization of our results, we conduct experiments on 7 public tabular datasets frequently used in fairness research. For unstructural datasets, such as images or texts, the key aspect is to design reasonable attribute flip methods before applications of MAFT. We refer interested readers to related works adapted for images[28–30] and texts[31–33], which could be integrated with our method. In addition, we have only tested fully-connected networks, since the shallow fully-connected

networks are good enough to accomplish the subject prediction tasks. Theoretically, MAFT is applicable for testing of more complicated models, like CNNs or RNNs, if the tested models are differentiable or differentiable almost everywhere. We will extend MAFT to unstructural datasets with diverse model architectures in future. For the strict settings where predicted probabilities are not available, a simple but coarse solution is to substitute the probability vector with a one-hot vector, of which the element corresponding to the predicted label is set to 1, and more sophisticated tricks need to be explored in future.

## 5 RELATED WORK

*Fair Deep Learning.* Recently, many literatures have identified several causes that can lead to unfairness in Deep Learning, including data and model. Many papers have proposed mechanisms to improve the fairness of ML algorithms. These mechanisms are typically categorised into three types [9]: pre-processing[34–38], in-processing[39–43], and post-processing[44–47]. There are also some fairness research focusing on specific domains, such as news recommendation[48] and recruitment[49, 50].

*Fairness Testing.* Bias in software is a prevalent issue, even when fairness is explicitly considered during the design process. Therefore, conducting fairness testing is a crucial step before deployment[11, 13]. Some works highly relative to this work have been introduced in Section 2. In addition to those, there are also some other works. Zheng et al. [29] proposed a white-box fairness testing method NeuronFair which can handle both structured and unstructured data and quantitatively interpret DNNs fairness violations. Ma et.al [51] introduced a seed selection approach I&D focusing on generating effective initial individual discriminatory instances to enhance fairness testing.

## 6 CONCLUSION

We propose a novel black-box individual fairness testing method called Model-Agnostic Fairness Testing (MAFT). MAFT allows practitioners to effectively identify and address discrimination in DL models, regardless of the specific algorithm or architecture employed. The experimental results demonstrate that MAFT achieves the same effectiveness as state-of-the-art white-box methods whilst improving the applicability to large-scale networks. Compared to existing black-box approaches, our approach demonstrates distinguished performance in discovering fairness violations w.r.t effectiveness ( $\sim 14.69\times$ ) and efficiency ( $\sim 32.58\times$ ).

## ACKNOWLEDGMENTS

This work is jointly supported by the NSFC-ISF Project (No. 62161146001) and the 'Digital Silk Road' Shanghai International Joint Lab of Trustworthy Intelligent Software (No. 22510750100), with additional funding from the Shanghai Trusted Industry Internet Software Collaborative Innovation Center. Additionally, we express our sincere thanks to Lingfeng Zhang, the first author of the EIDIG work, for his invaluable assistance in refining our experiments and improving academic manuscript during the revision process.

## REFERENCES

- [1] Andre Esteva, Alexandre Robicquet, Bharath Ramsundar, Volodymyr Kuleshov, Mark DePristo, Katherine Chou, Claire Cui, Greg Corrado, Sebastian Thrun, and Jeff Dean. A guide to deep learning in healthcare. *Nature medicine*, 25(1):24–29, 2019.
- [2] James B Heaton, Nick G Polson, and Jan Hendrik Witte. Deep learning for finance: deep portfolios. *Applied Stochastic Models in Business and Industry*, 33(1):3–12, 2017.
- [3] Myeongsuk Pak and Sanghoon Kim. A review of deep learning in image recognition. In *2017 4th international conference on computer applications and information processing technology (CAIPT)*, pages 1–3. IEEE, 2017.
- [4] Xiaoli Ren, Xiaoyong Li, Kaijun Ren, Junqiang Song, Zichen Xu, Kefeng Deng, and Xiang Wang. Deep learning-based weather prediction: a survey. *Big Data Research*, 23:100178, 2021.
- [5] Ian J Goodfellow, Jonathon Shlens, and Christian Szegedy. Explaining and harnessing adversarial examples. *arXiv preprint arXiv:1412.6572*, 2014.
- [6] Alexey Kurakin, Ian Goodfellow, Samy Bengio, et al. Adversarial examples in the physical world, 2016.
- [7] Nicolas Papernot, Patrick McDaniel, Somesh Jha, Matt Fredrikson, Z Berkay Celik, and Ananthram Swami. The limitations of deep learning in adversarial settings. In *2016 IEEE European symposium on security and privacy (EuroS&P)*, pages 372–387. IEEE, 2016.
- [8] Christian Szegedy, Wojciech Zaremba, Ilya Sutskever, Joan Bruna, Dumitru Erhan, Ian Goodfellow, and Rob Fergus. Intriguing properties of neural networks. *arXiv preprint arXiv:1312.6199*, 2013.
- [9] Dana Pessach and Erez Shmueli. A review on fairness in machine learning. *ACM Computing Surveys (CSUR)*, 55(3):1–44, 2022.
- [10] Dwork Cynthia, Hardt Moritz, Pitassi Toniann, Reingold Omer, and Zemel Richard. Fairness through awareness. In *Proceedings of the 3rd innovations in theoretical computer science conference*, number ITCS'12, pages 214–226. Association for Computing Machinery, New York, NY, USA, 2012.
- [11] Sainyam Galhotra, Yuriy Brun, and Alexandra Meliou. Fairness testing: testing software for discrimination. In *Proceedings of the 2017 11th joint meeting on foundations of software engineering*, pages 498–510, 2017.
- [12] Aniya Agarwal, Pranay Lohia, Seema Nagar, Kuntal Dey, and Diptikalyan Saha. Automated test generation to detect individual discrimination in ai models. *arXiv preprint arXiv:1809.03260*, 2018.
- [13] Marianne Huchard, Christian Kästner, and Gordon Fraser. Proceedings of the 33rd acm/ieee international conference on automated software engineering (ase 2018). In *ASE: Automated Software Engineering*. ACM Press, 2018.
- [14] Aniya Aggarwal, Pranay Lohia, Seema Nagar, Kuntal Dey, and Diptikalyan Saha. Black box fairness testing of machine learning models. In *Proceedings of the 2019 27th ACM Joint Meeting on European Software Engineering Conference and Symposium on the Foundations of Software Engineering*, pages 625–635, 2019.
- [15] Peixin Zhang, Jingyi Wang, Jun Sun, Guoliang Dong, Xinyu Wang, Xingen Wang, Jin Song Dong, and Ting Dai. White-box fairness testing through adversarial sampling. In *Proceedings of the ACM/IEEE 42nd International Conference on Software Engineering*, pages 949–960, 2020.
- [16] Lingfeng Zhang, Yueling Zhang, and Min Zhang. Efficient white-box fairness testing through gradient search. In *Proceedings of the 30th ACM SIGSOFT International Symposium on Software Testing and Analysis*, pages 103–114, 2021.
- [17] Yinpeng Dong, Fangzhou Liao, Tianyu Pang, Hang Su, Jun Zhu, Xiaolin Hu, and Jianguo Li. Boosting adversarial attacks with momentum. In *Proceedings of the IEEE conference on computer vision and pattern recognition*, pages 9185–9193, 2018.
- [18] Chuan Guo, Jacob Gardner, Yurong You, Andrew Gordon Wilson, and Kilian Weinberger. Simple black-box adversarial attacks. In *International Conference on Machine Learning*, pages 2484–2493. PMLR, 2019.
- [19] Pin-Yu Chen, Huan Zhang, Yash Sharma, Jinfeng Yi, and Cho-Jui Hsieh. Zoo: Zeroth order optimization based black-box attacks to deep neural networks without training substitute models. In *Proceedings of the 10th ACM workshop on artificial intelligence and security*, pages 15–26, 2017.
- [20] Ian Goodfellow, Yoshua Bengio, and Aaron Courville. *Deep learning*. MIT press, 2016.
- [21] Stuart Lloyd. Least squares quantization in pcm. *IEEE transactions on information theory*, 28(2):129–137, 1982.
- [22] Boris T Polyak. Some methods of speeding up the convergence of iteration methods. *Ussr computational mathematics and mathematical physics*, 4(5):1–17, 1964.
- [23] W Duch and J Korczak. Optimization and global minimization methods suitable for neural networks, neural computing surveys, 1999.
- [24] Mengnan Du, Fan Yang, Na Zou, and Xia Hu. Fairness in deep learning: A computational perspective. *IEEE Intelligent Systems*, 36(4):25–34, 2020.
- [25] Ellen R Girden. *ANOVA: Repeated measures*. Number 84. Sage, 1992.
- [26] Student. The probable error of a mean. *Biometrika*, pages 1–25, 1908.
- [27] Andrzej Maćkiewicz and Waldemar Ratajczak. Principal components analysis (pca). *Computers & Geosciences*, 19(3):303–342, 1993.
- [28] Peixin Zhang, Jingyi Wang, Jun Sun, and Xinyu Wang. Fairness testing of deep image classification with adequacy metrics. *arXiv preprint arXiv:2111.08856*, 2021.
- [29] Haibin Zheng, Zhiqing Chen, Tianyu Du, Xuhong Zhang, Yao Cheng, Shouling Ji, Jingyi Wang, Yue Yu, and Jinyin Chen. Neuronfair: Interpretable white-box fairness testing through biased neuron identification. In *Proceedings of the 44th International Conference on Software Engineering*, pages 1519–1531, 2022.
- [30] Yisong Xiao, Aishan Liu, Tianlin Li, and Xianglong Liu. Latent imitator: Generating natural individual discriminatory instances for black-box fairness testing. *arXiv preprint arXiv:2305.11602*, 2023.
- [31] Pingchuan Ma, Shuai Wang, and Jin Liu. Metamorphic testing and certified mitigation of fairness violations in nlp models. In *IJCAI*, pages 458–465, 2020.
- [32] Ezekiel Soremekun, Sakshi Udeshi, and Sudipta Chattopadhyay. Astraea: Grammar-based fairness testing. *IEEE Transactions on Software Engineering*, 48(12):5188–5211, 2022.
- [33] Ming Fan, Wenying Wei, Wuxia Jin, Zijiang Yang, and Ting Liu. Explanation-guided fairness testing through genetic algorithm. In *Proceedings of the 44th International Conference on Software Engineering*, pages 871–882, 2022.
- [34] Flavio Calmon, Dennis Wei, Bhanukiran Vinzamuri, Karthikeyan Natesan Ramamurthy, and Kush R Varshney. Optimized pre-processing for discrimination prevention. *Advances in neural information processing systems*, 30, 2017.
- [35] Joel Escudé Font and Marta R Costa-Jussa. Equalizing gender biases in neural machine translation with word embeddings techniques. *arXiv preprint arXiv:1901.03116*, 2019.
- [36] Christos Louizos, Kevin Swersky, Yujia Li, Max Welling, and Richard Zemel. The variational fair autoencoder. *arXiv preprint arXiv:1511.00830*, 2015.
- [37] Samira Samadi, Uthaipon Tantipongpipat, Jamie H Morgenstern, Mohit Singh, and Santosh Vempala. The price of fair pca: One extra dimension. *Advances in neural information processing systems*, 31, 2018.
- [38] Rich Zemel, Yu Wu, Kevin Swersky, Toni Pitassi, and Cynthia Dwork. Learning fair representations. In *International conference on machine learning*, pages 325–333. PMLR, 2013.
- [39] Alekh Agarwal, Alina Beygelzimer, Miroslav Dudík, John Langford, and Hanna Wallach. A reductions approach to fair classification. In *International conference on machine learning*, pages 60–69. PMLR, 2018.
- [40] Yahav Bechavod and Katrina Ligett. Learning fair classifiers: A regularization-inspired approach. *arXiv preprint arXiv:1707.00044*, pages 1733–1782, 2017.
- [41] Yahav Bechavod and Katrina Ligett. Penalizing unfairness in binary classification. *arXiv preprint arXiv:1707.00044*, 2017.
- [42] Toon Calders and Sicco Verwer. Three naive bayes approaches for discrimination-free classification. *Data mining and knowledge discovery*, 21:277–292, 2010.
- [43] Gabriel Goh, Andrew Cotter, Maya Gupta, and Michael P Friedlander. Satisfying real-world goals with dataset constraints. *Advances in neural information processing systems*, 29, 2016.
- [44] Sam Corbett-Davies, Emma Pierson, Avi Feller, Sharad Goel, and Aziz Huq. Algorithmic decision making and the cost of fairness. In *Proceedings of the 23rd acm sigkdd international conference on knowledge discovery and data mining*, pages 797–806, 2017.
- [45] Cynthia Dwork, Nicole Immorlica, Adam Tauman Kalai, and Max Leiserson. Decoupled classifiers for group-fair and efficient machine learning. In *Conference on fairness, accountability and transparency*, pages 119–133. PMLR, 2018.
- [46] Moritz Hardt, E Price, N Srebro, D Lee, M Sugiyama, U Luxburg, I Guyon, and R Garnett. Advances in neural information processing systems. 2016.
- [47] Chandler May, Alex Wang, Shikha Bordia, Samuel R Bowman, and Rachel Rudinger. On measuring social biases in sentence encoders. *arXiv preprint arXiv:1903.10561*, 2019.
- [48] Chuhan Wu, Fangzhao Wu, Xiting Wang, Yongfeng Huang, and Xing Xie. Fairness-aware news recommendation with decomposed adversarial learning. In *Proceedings of the AAAI Conference on Artificial Intelligence*, volume 35, pages 4462–4469, 2021.
- [49] Vitalii Emelianov, Nicolas Gast, Krishna P Gummadi, and Patrick Loiseau. On fair selection in the presence of implicit variance. In *Proceedings of the 21st ACM Conference on Economics and Computation*, pages 649–675, 2020.
- [50] Vitalii Emelianov, Nicolas Gast, Krishna P Gummadi, and Patrick Loiseau. On fair selection in the presence of implicit and differential variance. *Artificial Intelligence*, 302:103609, 2022.
- [51] Minghua Ma, Zhao Tian, Max Hort, Federica Sarro, Hongyu Zhang, Qingwei Lin, and Dongmei Zhang. Enhanced fairness testing via generating effective individual discriminatory instances. *arXiv preprint arXiv:2209.08321*, 2022.